UCRL- 85577 Rev. 1
PREPRINT
CONF-810442--2(Rev.1)

MASTER

MOLECULAR POTENTIALS AND RELAXATION DYNAMICS

Arnold M. Karo

THIS PAPER WILL BE PUBLISHED AS PART OF THE
PROCEEDINGS OF THE UNITED STATES NATIONAL SCIENCE
FOUNDATION AND THE MEXICAN NATIONAL COUNCIL OF
SCIENCE AND TECHNOLOGY WORKSHOP ON NEGATIVE IONS
San Juan Del Rio, Queretaro, Mexico
April 1 - April 4, 1981

May 18, 1981

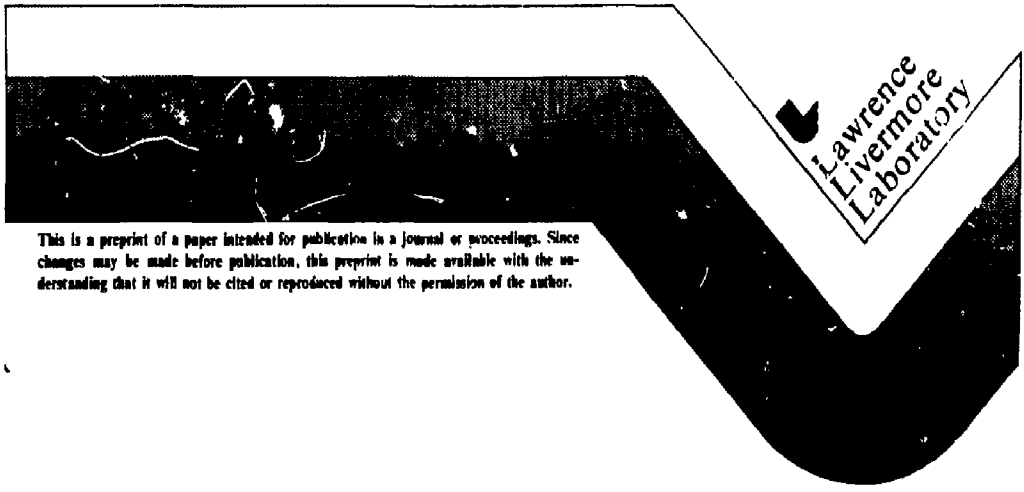

MOLECULAR POTENTIALS AND RELAXATION DYNAMICS*

Arnold M. Karo
Lawrence Livermore National Laboratory
University of California
Livermore, CA 94550

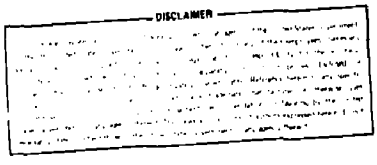

*Work performed under the auspices of the U. S. Department of Energy by the Lawrence Livermore National Laboratory under contract number W-7405-ENG-48.

ABSTRACT

The use of empirical pseudopotentials, in evaluating interatomic potentials, provides an inexpensive and convenient method for obtaining highly accurate potential curves and permits the modeling of core-valence correlation, and the inclusion of relativistic effects when these are significant. We will discuss as an example our recent calculations of the $X^1\Sigma^+$ and $a^3\Sigma^+$ states of LiH, NaH, KH, RbH, and CsH and the $X^2\Sigma^+$ states of their anions. Pseudopotentials, including core polarization terms, have been used to replace the core electrons, and this has been coupled with the development of compact, highly-optimized basis sets for the corresponding one- and two-electron atoms. Comparisons of the neutral potential curves with experiment and other ab initio calculations show good agreement (within 1000 cm^{-1} over most of the potential curves) with the difference curves being considerably more accurate.

In the method of computer molecular dynamics, the force acting on each particle is the resultant of all interactions with other atoms in the neighborhood and is obtained as the derivative of an effective many-body potential. Exploiting the pseudopotential approach, in obtaining the appropriate potentials may be very fruitful in the future. In the molecular dynamics example we consider here, we use, however, the conventional sum-of-pairwise-interatomic-potentials (SPP) approximation with the potentials derived either from experimental spectroscopic data or from Hartree-Fock calculations. The problem is the collisional de-excitation of vibrationally excited molecular hydrogen at an Fe surface. Our calculations have been carried out for an initial vibrotational state $v = 8$, $J = 1$ and a translational temperature corresponding to a gas temperature of 500 K. Different angles of approach and different initial random impact points on the surface have been selected. For any given collision with the wall, the molecule may pick up or lose vibrotational and translational energy. Averaging of the results of many trajectory runs has been carried out in order to arrive at meaningful conclusions about the probability of de-excitation as a function of such parameters as the number of wall collisions, the residence time, the wall temperature, and the microscopic nature of the wall itself.

I. INTRODUCTION

Satisfactory progress in the development of present designs for negative ion sources depends on a thorough understanding of the physical processes involved in three general areas: double charge-exchange processes such as occur when protons are passed through an alkali vapor; electron-volume processes in which low-energy electrons interact with molecular species, leading to negative ion products by means of recombination or dissociative attachment; and the generation of negative ions in surface interactions, mainly by means of desorption and backscattering. The theory of charge-exchange processes in metal vapor targets is not well-developed, but at the low energies appropriate to alkali charge exchange, the relevant potentials are the alkali hydride potentials which must be known to high accuracy. Accurate negative-ion and neutral-molecule interatomic potential energies are also needed for the development of mechanisms that can explain the enhanced production of negative ions by particle bombardment of alkali-coated metal surfaces. Here, incident energetic protons are backscattered as hydrogen anions from the cathode substrate with an appreciable fraction of their incident energy.[1] We have proposed[2] that hydrogen negative ions may be perferentially formed by means of an electron-transfer process during the interaction of H atoms with Cs atoms that are absorbed on the W cathode, in a region several angstroms in front of the surface. The cross-section or probability of the transfer process occurring should depend strongly on the relative position of the alkali hydride neutral and negative ion potential energies.

Finally, in the area concerning electron-volume processes, we will consider the scattering of vibrationally excited hydrogen molecules from a wall of iron atoms. The force acting on each particle is the resultant of all interactions with other atoms and is the derivative of an effective many-body potential. In our treatment we will use a sum of pairwise interatomic potentials, with the potentials derived either from experimental spectroscopic data or from Hartree-Fock calculations. Thus at this level of approximation we return again to the problem of evaluating accurate pair potentials.

II. MC-SCF PSEUDOPOTENTIAL CALCULATIONS OF THE POTENTIALS RELEVANT TO DOUBLE CHARGE EXCHANGE AND PLASMA-SURFACE INTERACTIONS.

There is a need for the accurate evaluation of the ground and low-lying electronic states of the alkali hydride negative ions and their parent neutral molecules over a wide range of internuclear separations because of the direct application of these results to the magnetic fusion energy program through ion source and injection technology. The calculation of electron affinities from such data is important in many areas where charge-transfer processes on atomic and molecular scales play a critical role. For example, accurate values of the molecular electron affinities over the entire range of internuclear separations are crucial for the hydrogen backscattering calculations of electron capture and loss probabilities.[2]

In earlier work on the alkali hydride neutral molecules and their negative ions[3] we carried out all-electron ab initio multi-configuration self consistant field (MC-SCF) calculations of the ground state potential energy curves for LiH, LiH^-, NaH, NaH^-, CsH and CsH^- over a range of internuclear distances. The evaluation of the LiH and LiH^- potentials inexpensively explored configurations contributing significantly to charge redistribution and electron correlation during bond formation and dissociation. The use of augmented double-zeta basis sets gave a good description of the neutral molecules and their negative ions. It was not possible to build more complexity into the basis sets because of limitations on the number of basis functions permitted by the CDC-7600 version of the computer code in use at that time.

Conventional Hartree-Fock self-consistent field (HF-SCF) procedures were used to evaluate the ground eigenstates for each neutral molecule AH ($X^1\Sigma^+$) and each negative ion AH^- ($X^2\Sigma^+$). The essence of the MC-SCF technique is summarized in the equations

$$H\Psi = E\Psi ,$$

$$\Psi(1,2,\ldots,N) = \Sigma_a A_a \Phi_a (1,2,\ldots,N).$$

Each configuration Φ_a consists of a distribution of the N electrons among some set of orthonormal orbitals ϕ_i, where

$$\Phi_a\,(1,2,....N) = \theta_{L,S}\,\phi_1\,(1)\,\phi_2\,(2)...\phi_N\,(N).$$

The symbol $\theta_{L,S}$ indicates projection to an eigenfunction of total angular momentum and spin. Each orbital is expanded in terms of basis functions χ:

$$\phi_i = \sum_p C_{ip}\chi_p,$$

so that the calculations are carried out within the framework of a conventional linear combination of atomic orbitals-molecular orbital (LCAO-MO) treatment. Logistically, the equations are solved by means of the following steps:

(1) A set of configurations Φ_a is chosen and initial guesses are made for the expansion coefficients C_{ip} in the ϕ_i (orbital) expansions.

(2) The configuration-mixing coefficients A_a are determined by diagonalizing the usual secular matrix.

(3) A new set of orbitals ϕ_i are determined by means of variational SCF procedures.

(4) Steps (2) and (3) are repeated iteratively until the entire process converges, so that the mixing coefficients A_a and orbitals ϕ_i are simultaneously optimized.

An accurate description of the interatomic potential between an alkali atom and H or H^- must take into account polarization effects and charge transfer. In this regard, it is important that the electron affinity of each atomic species be calculated accurately.

In comparing our results for the molecular electron affinity for NaH at the equilibrium distance of the neutral molecule with those of Griffing, et al[4] and Olson and Liu[5] (0.278eV versus 0.3618 eV and 0.373eV) it is most likely that the bulk of the difference can be ascribed to the use of a less than optimum basis and the neglect of core-valence correlation. This latter error becomes more marked for heavier alkalis and will have a significant effect on the polarizabilities of these atoms. Thus, although the basis sets for the

all-electron ab initio calculations were carefully chosen to allow for a good description of the neutral and negative ion systems, the constraints alluded to earlier imposed by the computer code underscores the need for a different approach that can be applied systematically to the heavier alkalis.

Calculations using empirical pseudopotentials permit the modeling of core-valence correlation and the inclusion of relativistic effects. Compact, highly-optimized basis sets for the resulting one- or two-electron atoms allow us to reproduce the atomic polarizabilities accurately. Overall, the accuracy of the present calculations is superior to our earlier ab initio work and gives a consistent representation of the molecules down the column of the periodic table. Where comparisons are possible, we find our results to be accurate to about 1000 cm^{-1} over most of the potential curves, with the difference curves being considerably more accurate.

A. METHOD OF CALCULATION

1. Pseudopotentials

The fact that the alkali atoms have only one valence electron makes them particularly suitable for the development of empirical core potentials which model the interactions of the valence and core electrons. Such potentials have been given by Bardsley.[6] The potentials are obtained by solving the one-electron radial equation.

$$\left[-\frac{1}{2}\nabla^2 - \frac{1}{r} + \frac{\ell(\ell+1)}{2r^2} + V_\ell^{core}(r)\right]\phi_\ell(r) = \epsilon_\ell \phi_\ell(r) \qquad (1)$$

for an assumed form of V_ℓ^{core} and comparing the calculated eigenvalues with the experimentally observed spectrum. V_ℓ^{core} is then adjusted until agreement between the calculated and observed valence spectrum is achieved.

The form of the potentials given by Bardsley is

$$V_\ell^{core} = A_\ell e^{-\gamma_\ell r^2} - \frac{\alpha_D}{2(r^2+d^2)^2} - \frac{\alpha_Q}{2(r^2+d^2)^3} \qquad (2)$$

The first term in eqn. 2 is repulsive for $\ell \leq \ell_{max}$ where ℓ_{max} is the highest ℓ quantum number occurring in the core. It represents the orthogonality of the valence electrons with the core and prevents the collapse of the valence orbitals into the core region. For $\ell > \ell_{max}$ the first term is attractive and represents the unshielding of the positively charged nucleus as the valence electron penetrates the core region.

The second and third terms in eqn. 2 represent an attempt to model core polarization effects. α_D and α_Q are the core dipole and quadrupole polarizabilities respectively. The d parameter in the denominators is a cutoff radius which approximates the radial extent of the core electronic distribution. The polarizabilities and the cutoff radii are not dependent on the ℓ quantum number. No provision has been made for polarization of the alkali cores by the proton in the hydride calculations. Corrections for this effect have been proposed,[7] but have not been used in the current calculations.

The parameters A_ℓ, γ_ℓ, α_D, α_Q, and d are varied to fit the observed atomic spectra (term values - ionization potential). For the alkalis, the spectra can be fitted to within a few wavenumbers with the potential given in eqn. 1. The optimized parameters have been reported by Bardsley[6] and are given in Table I.

The use of empirical pseudopotentials in calculations involving alkalis offers several important advantages. The foremost is the reduction of a many-electron problem to one containing only a few electrons. The size of the basis set is greatly reduced due to the nodeless nature of the atomic pseudo-orbitals. This results in a drastic reduction in computer time versus an all-electron calculation. Another advantage arises through the inclusion of core polarization effects. This allows the energies and ionization potentials of the alkalis to be obtained accurately without large core-valence configuration interaction. Core polarizability plays a significant role in the heavier alkalis, not only in the energies and ionization

Table I. Pseudopotential Parameters Used in the Calculations (Taken from Ref. 6). The Form of the Potentials is

$$V(r) = \sum_{\ell}^{\ell_{max}} V_\ell(r) = \sum_{\ell}^{\ell_{max}} A_\ell e^{-\gamma_\ell r^2} - \frac{\alpha_D}{(r^2+d^2)^2} - \frac{\alpha_Q}{(r^2+d^2)^3}$$

	Li	Na	K	Rb	Cs
α_D	0.1925	0.945	5.47	8.966	15.0
α_Q	0.112	5.0	41.5	102.0	230.0
d	0.75	1.1	1.5	1.95	2.0
ℓ_{max}	2	2	2	2	2
A_0	6.013668	10.28159	9.568369	17.29503	14.76732
γ_0	1.293213	1.294506	0.709742	0.746748	0.541614
A_1	-0.740679	2.692467	2.897295	2.851747	2.960707
γ_1	1.410279	0.681447	0.363969	0.295391	0.232594
A_2	-0.067342	-1.452763	-3.916641	-1.553162	-0.399982
γ_2	0.8	1.0	0.748353	0.387761	0.193255

potentials, but also in the atomic polarizabilities. A third advantage of the empirically derived potentials is that they implicitly include the effects of relativistic contraction of the core electronic distribution. This is only important for the Cs atom, where it has the effect of reducing the radial extend of the 6s orbital by about 10%.

The major disadvantage of the model potentials arises in molecular calculations at smaller internuclear separations where two-center core-core interactions become important. This effect is minimal in the case of the hydrides, but we would expect the proton-alkali core interaction to begin to deviate from the assumed 1/R repulsion at small internuclear distances.

2. Basis Set Development

For the calculations described here, we developed very compact basis sets which are still flexible enough to describe the relevant physics of the alkali hydrides and their negative ions. The criteria for basis set choice included the ionization potential, electron affinity, and dipole polarizability of each atom.

The hydrogen basis set was constructed by optimizing two 1s functions to get the lowest single-configuration energy for H^-. This double-zeta basis was then augmented with functions of the next higher n and l quantum numbers to permit an adequate multiconfiguration description of the anion. Screening constants for the 2s and 2p functions were also chosen to have maximum radial overlap with the 1s orbital. One additional 2p Slater-type orbital (STO) was added to the basis to improve the single-configuration self-consistent-field (SC-SCF) dipole polarizability of H^-. This results in 5 basis functions which give a reasonable description of H^- at the four configuration level, and the dipole polarizabilities of H and H^- at the SC-SCF level.

Basis sets for the alkalis were developed by first optimizing the exponents of a triple-zeta set of s STO's for the ground state energy. To this basis a fourth s STO was added and optimized to give the lowest

energy for the negative atom in a SC-SCF calculation. Two p polarization functions were then added and optimized; one for the neutral ground state dipole polarizability and one for the anion ground state polarizability in the SC-SCF approximation.

The final basis sets are shown in Table II. The values of the properties used as criteria for basis set optimization are shown in Table III along with accurate comparison values. It is interesting to note that all-electron ab initio polarizabilities for the alkalis, if core polarization effects are neglected, are much larger than the present values.

There is some room for basis set improvement in future calculations. First, the electron affinities would be improved by adding d functions to the bases and increasing the number of configurations from four to seven. Second, the alkali bases could be improved by adding d and f functions optimized for the quadrupole and octupole polarizabilities. These higher order terms can play a significant role in the polarization of the alkalis by H^-, particularly at small internuclear separations.[8]

3. Description of the Wavefunctions

In calculations on any molecular state that develops significant charge-transfer character, the energetic splitting of the neutral and charge-transfer asymptotes must be accurately described. For the alkali hydrides, our four-configuration wavefunctions give asymptotic energies which are within 0.1eV of their experimental values. A minimum of two configurations is necessary to describe the dissociation of the $^1\Sigma^+$ ground states into two ^2S atoms; an additional two configurations are necessary to yield an adequate correlated description of H^- in the charge-transfer region. Thus, for the neutral alkali hydrides, four configuration wavefunctions are optimized at each nuclear separation by multi-configuration self-consistent-field (MC-SCF) techniques.[9] The form of the wavefunction is $1\sigma^2 + 2\sigma^2 + 3\sigma^2 + 1\pi^2$, where the orbital numbering begins with 1σ and 1π because the core electrons are not explicitly considered.

Table II. Slater-Type Orbital (STO) Basis Sets

Exponents

STO	H(n=1)	Li(n=2)	Na(n=3)	K(n=4)	Rb(n=5)	Cs(n=6)
(n-1)s		0.41204	0.79010	1.13458	1.47256	1.61996
ns	1.21809	1.61033	2.48718	1.13377	1.45575	1.56901
ns'	0.46290	0.73170	0.69383	0.68929	0.83134	0.90516
ns''		0.30000	0.37188	0.39375	0.45312	0.49375
(n+1)s	1.05794					
np		2.01303	0.72147	0.81999	1.06297	1.19961
(n+1)p	1.05794					
np'		0.50055	0.55785	0.55605	0.67145	0.74257
(n+1)p'	0.30937					

Table III. Atomic Ionization Potentials, Electron Affinities, and Dipole Polarizabilities

Species	I.P.(eV) Accurate	I.P.(eV) Calc.	E.A.(eV) Accurate[d]	E.A.(eV) Calc.[b]	$\alpha_D(A^3)$ Recommended[c]	$\alpha_D(A^3)$ Calc.	Calc.[d]
H	13.60	13.605	0.754	0.665	0.67	0.59	
Li	5.39	5.386	0.620	0.624	24.3	24.63	
Na	5.14	5.137	0.546	0.561	23.6	24.77	27.70
K	4.34	4.327	0.501	0.555	43.4	46.88	
Rb	4.18	4.168	0.486	0.549	47.3	52.44	
Cs	3.89	3.889	0.472	0.547	59.6	67.43	110.20

[a] H. Hotop and W. C. Lineberger, J. Phys. Chem. Ref. Data 4, 539 (1975).

[b] Four configuration MCSCF.

[c] T. M. Miller and B. Bederson, Adv. Atom. Mol. Phys. 13, 1 (1977).

[d] All-electron ab initio results neglecting core polarization (Ref. 3).

The molecular anion ground states are a little simpler. Like other alkali-containing diatomic anions,[8] the potential curve is defined by the polarization of the alkali by H^-, which is overcome at smaller internuclear separations by repulsive overlap effects. The essential features of this interaction can be described at the SC-SCF level. However, the size and distortability of the H^- is quite sensitive to configuration interaction. In addition, for purposes of comparison with the neutral molecule, it is important that the anion be described at a similar level of accuracy. For this reason we use a four-configuration MC-SCF wavefunction for the anion ground states. The form of the wavefunction is $1\sigma^2 4\sigma + 2\sigma^2 4\sigma + 3\sigma^2 4\sigma + 1\pi^2 4\sigma$. The 4σ orbital represents the alkali valence electron while the remaining orbitals represent the correlated H^-.

Some improvement in the wavefunctions could be obtained if first-order configuration interaction (FOCI) is added. This allows for charge transfer plus polarization of the occupied valence orbitals. In the case of the anions, the effect is to enhance the interaction of the ground state with the state arising from the A^- +H asymptote. FOCI has not been included in the calculations reported here, so we might expect our anion ground states to be slightly less bound than they would be in a more complete CI treatment.

The triplet states of the neutral molecules, which arise from the same asymptote as the ground states, exhibit no bond formation. We have found that an SC-SCF calculation is adequate to describe the triplet interaction energy to within a few hundreths of an eV.

B. RESULTS

1. LiH and LiH^-

The lithium hydride molecule has been much studied theoretically. It has been used as a test molecule for just about every *ab initio* quantum mechanical method. Our discussion of LiH will be limited to a comparison with experiment[10] and a few very accurate *ab initio* calculations.[11,12,13]

In Fig. 1 we have plotted our results for the $X^1\Sigma^+$ and $^3\Sigma^+$ states of LiH and the $X^2\Sigma^+$ state of LiH^-. Also plotted are the all-electron calculated curves of Liu, et al[11], which are the most accurate results published to date. The spectroscopic constants derived from our curves are given in Table IV. The experimental RKR curve for LiH[10] is very close to the theoretical curve of Liu, et al, so it has not been plotted.

Of all the theoretical calculations for LiH in the literature, the configuration interaction calculations of Liu, O-Ohata, and Docken (LOD)[11] and Rosmus and Meyer (RM)[12] appear to be the most accurate. The LOD calculation was an extensive valence electron CI with an STO basis set that was carefully optimized for the atoms and the molecule. The reported dissociation energy (20066 cm^{-1}) differs from the experimental[14] (20286.6 cm^{-1}) by only 220 cm^{-1}. The RM calculation used a different CI technique that included core-valence CI. Their gaussian basis set was also very large, but not optimized to the same level as LOD. Their computed dissociation energy also is very near the experimental value, differing by only 320 cm^{-1}. The difference between our calculated $X^1\Sigma^+$ curve and these accurate determinations is due to limitations other than the use of a pseudopotential to replace the core electrons. First, our calculated electron affinity for hydrogen is too small by about 0.1 eV, which places the change transfer state too high asymptotically. Second, our basis set includes only dipole polarization functions on the hydrogen, which reduces the Li^+H^- interaction energy. Our final curve is about 1200 cm^{-1} more shallow than the best theoretical results. A single calculation near R_e which included the extra polarization functions used by LOD indicates that the error can be reduced by 30% by use of the more extensive basis.

A calculation of accuracy intermediate between ours and the two CI calculations is the 8 configuration MCSCF calculation of Docken and Hinze.[13] They used a large STO basis set which included p, d, and f polarization functions optimized at the R_e of the molecule. Their

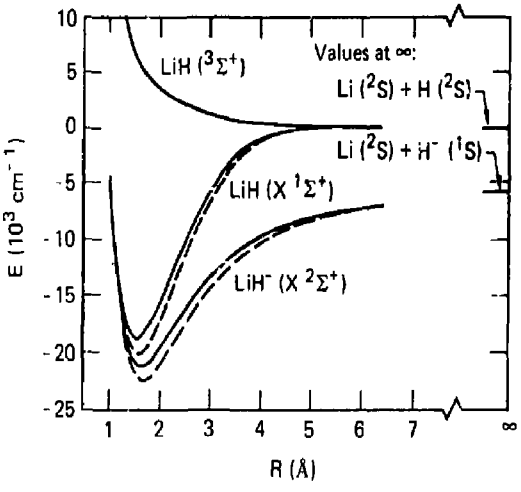
10
5
0
-5
-10
-15
-20
-25
E (10^3 cm^{-1})
1
2
3
4
5
6
7
∞
R (Å)
LiH ($^3\Sigma^+$)
Values at ∞:
Li (^{2}S) + H (^{2}S)
Li (^{2}S) + H$^-$ (^{1}S)
LiH (X $^1\Sigma^+$)
LiH$^-$ (X $^2\Sigma^+$)

Figure 1

calculated dissociation energy was 842 cm^{-1} less than the experimental value. Most of this error is due to the use of MCSCF orbitals simultaneously optimized for the ground state and the $A^1\Sigma^+$ excited state.

The three ab initio calculations described above required considerably more effort than our present calculations. However, with the compact basis set and wavefunctions we have chosen, the calculated dissociation energy is in error by only 6%, the predicted R_e is within 0.015 Å of the experimental value, and the value of ω_e is within 13 cm^{-1} of the accepted value.

For the $X^2\Sigma^+$ state of the LiH^- anion, we can again compare with the calculations of LOD.[11] In Fig. 1 we have chosen to shift our calculated asymptote to coincide with the experimental electron affinity of hydrogen. This shift seems justified, since the H^- remains intact over most of the range of interaction. Our predicted dissociation energy of 15146 cm^{-1} is 1500 cm^{-1} less than that of LOD as shown in Table IV. Four-configuration calculations near R_e with the additional p, d, and f polarization functions given by LOD, show that half of our error is due to the basis set. Our calculated adiabatic electron affinity for LiH is 0.293eV, which is close to the value of 0.318eV given by LOD. Rosmus and Meyer[15] have reported 0.26eV from their PNO-CI and CEPA calculations. Another value of 0.299eV has been determined by Griffing, et al[16] using an equations-of-motion method.

2. NaH and NaH^-

The Hartree-Fock ionization potential for sodium is 0.185eV[17] less than the experimental value. This measures directly the importance of core polarization in the sodium atom. Two previous NaH calculations have included core-valence CI. The first is due to RM[12] who used PNO-CI and CEPA methods similar to their calculations on LiH. Their computed dissociation energy of 15486 cm^{-1} is only 274 cm^{-1} less than the value of 15760 cm^{-1} deduced by Stwalley[17] from spectroscopic data. Our value of 15204 cm^{-1} as reported in Table IV

Table IV. Calculated Spectroscopic Constants for the $X\ ^1\Sigma^+$ States of the Alkali Hydrides Versus Experiment, and Calculated Spectroscopic Constants for the $X\ ^2\Sigma^+$ States of the Alkali Hydride Negative Ions Versus Other Theoretical Values.

Molecule		R_e(Å)	$D_e(cm^{-1})$[b]	$\omega_e(cm^{-1})$	$\omega_e x_e(cm^{-1})$	E.A. (eV)
LiH	Calc.	1.58	18861	1418.7	24.9	0.293
	Ref. 14	1.595	20286.6 ± .6	1406.10	23.195	
LiH⁻	Calc.	1.70	15146	1186.6	26.7	
	Ref. 11	1.69	16647	1167.6	28.3	
	Ref. 15	1.672	16397	1191.8	28.0	
NaH	Calc.	1.88	15204	1172.7	19.9	0.316
	(a)	1.887	15760 ± 300	1171.4	19.52	
NaH⁻	Calc.	1.98	11673	940.5	21.5	
	Ref. 5	2.04	12276	912.0		
	Ref. 15	2.012	12227	927	24	
KH	Calc.	2.24	14490	985.7	14.6	0.437
	Ref. 20	2.244	14550 ± 300	985.24	14.92	
KH⁻	Calc.	2.35	11937	809.5	16.6	
RbH	Calc.	2.30	14294	944.3	13.7	0.422
	Ref. 21	2.368	14240 ± 300	936.62	13.965	
RbH⁻	Calc.	2.44	11617	722.2	15.5	
CsH	Calc.	2.42	15384	942.8	13.1	0.438
	Ref. 22	2.494	15000 ± 500	891.0	12.93	
CsH⁻	Calc.	2.53	12835	971.5	14.7	

[a] E.S. Sachs, J. Hinze, and N. H. Sabelli, J. Chem. Phys. 62, 3367 (1975).

[b] Experimentally estimated dissociation energies for NaH, KH, and RbH from Ref. 17; the experimental D_e for CsH taken from Ref. (a), this table.

is surprisingly close to the Rosmus and Meyer results in light of the errors discussed previously for LiH. Another accurate all-electron calculation on NaH has been reported recently by Olson and Liu.[5] Their dissociation energy (15502 cm^{-1}), which they estimate to be within 200 cm^{-1} of the correct value, is very close to that of Rosmus and Meyer[12] and experiment and only slightly larger than our value. In addition, all three theoretical calculations yield spectroscopic constants in very good agreement with experiment.[18] Our calculated potential curves for the $X^1\Sigma^+$ and $^3\Sigma^+$ states are compared to Olson and Liu[5] in Fig. 2.

Since our NaH calculations were carried out with basis sets and wavefunctions developed identically to those used for LiH, one would expect the inherent errors in the two calculations to be similar. However, NaH includes significant core polarization effects which are negligible in LiH, and which have not been corrected for proton-core polarization interactions in our calculations. As shown in the next section, the lack of core-core corrections tends to artifically deepen and skew the calculated potential curves. Our $^3\Sigma^+$ curve, which contains minimal errors due to basis set and wavefunction limitations, should give an indication of the proton-core interaction errors. In Fig. 2 we have compared our $^3\Sigma^+$ curve to Olson and Liu.[5] Near the R_e of the ground state, our $^3\Sigma^+$ interaction energy is 750 cm^{-1} less than theirs. If our ground state D_e is reduced by this amount, we find that our computed binding is about 1000 cm^{-1} less than either Olson and Liu[5] or Rosmus and Meyer.[12] This is very similar to the error found in LiH and supports a value of approximately 15500 cm^{-1} for the true NaH dissociation energy.

Our calculated potential curve for NaH^- is shown in Fig. 2 and the spectroscopic constants are given in Table IV. If the anion curve is shifted to account for the asymptotic error of 0.089eV in the electron affinity of hydrogen, we obtain an electron affinity for NaH of 0.316eV calculated from the minima of the potential curves. This is slightly larger than our previously reported[3] value of 0.278eV from

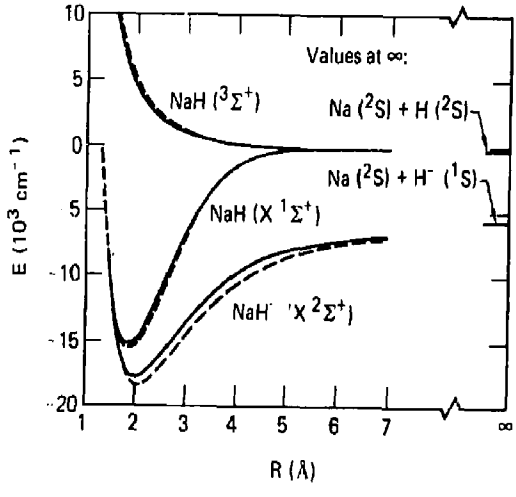
10
5
0
5
-10
-15
-20
1
2
3
4
5
6
7
∞
E (10^3 cm^{-1})
R (Å)
Values at ∞:
NaH ($^3\Sigma^+$)
Na (^{2}S) + H (^{2}S)
Na (^{2}S) + H$^-$ (^{1}S)
NaH (X $^1\Sigma^+$)
NaH$^-$ (X $^2\Sigma^+$)

Figure 2

all-electron MCSCF calculations. Olson and Liu[5] predict a value of 0.373eV from their large-scale CI calculations. Our potential energy curve for the $X^2\Sigma^+$ state is compared to Olson and Liu in Fig. 2. The disagreement in the anion curves is larger than the differences noted for the neutral curve. The Olson and Liu calculation for the negative ion did not include core-valence CI, which implies that their polarizabilities for sodium are too large and, consequently, their binding energy is probably slightly too large. Rosmus and Meyer[15] have also performed an all-electron calculation of the E.A. of NaH including core-valence CI. Their value of 0.31eV is close to ours. Jordan, et al,[4,16] report a value of 0.36eV from an equations-of-motion calculation.

3. KH, KH^-, RbH, RbH^-, CsH, and CsH^-

The potential energy curves for the heavier alkali hydrides and their anions are shown in Figs. 3-5. For these heavier systems there are no accurate all-electron calculations with which to compare. However, there are RKR potentials[19-21] and estimated dissociation energies[17,22] for the neutral ground states. From Table IV we see that our calculated spectroscopic constants are in excellent agreement with the experimental values. There is a tendency for the R_e values to become too small and the ω_e values to become too large as we go from KH to CsH. This is to be expected, since the core polarization effects become more significant as we go down the group and the uncorrected proton-core interactions introduce larger errors. The $^3\Sigma^+$ states become less repulsive in going from KH to CsH, with CsH showing a distinct potential minimum. This minimum is not expected from a single configuration calculation, and is almost certainly due to the incorrect proton-core interaction.

For the negative ion states, we have no data with which to compare our calculations. Recalling that the errors in the neutral and negative ion states for LiH and NaH are comparable, we can expect that our predicted E.A.'s for the heavier systems are reasonably accurate. Our calculations yield 0.44, 0.42, and 0.44 for the E.A.'s of KH, RbH, and

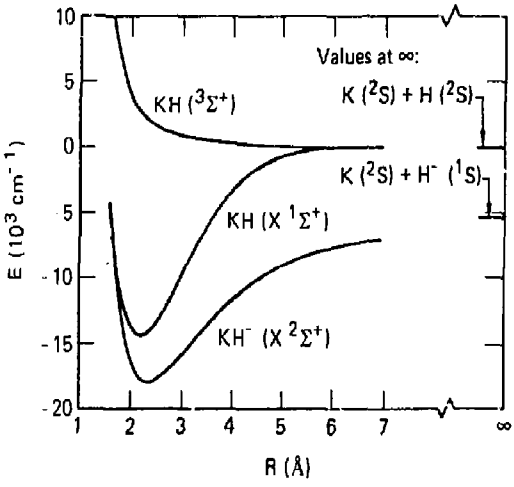
10
5
0
-5
-10
-15
-20
E (10^3 cm^{-1})
1
2
3
4
5
6
7
∞
R (Å)
Values at ∞:
K (^{2}S) + H (^{2}S)
K (^{2}S) + H$^-$ (^{1}S)
KH ($^3\Sigma^+$)
KH ($X\,^1\Sigma^+$)
KH$^-$ ($X\,^2\Sigma^+$)

Figure 3

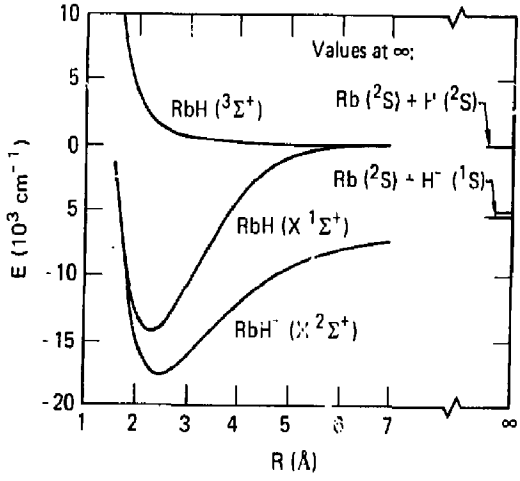
10
5
0
5
-10
-15
-20
E (10^3 cm^{-1})
1
2
3
4
5
6
7
∞
R (Å)
Values at ∞:
RbH ($^3\Sigma^+$)
Rb (^{2}S) + H$^+$ (^{2}S)
Rb (^{2}S) + H$^-$ (^{1}S)
RbH (X $^1\Sigma^+$)
RbH$^-$ (X $^2\Sigma^+$)

Figure 4

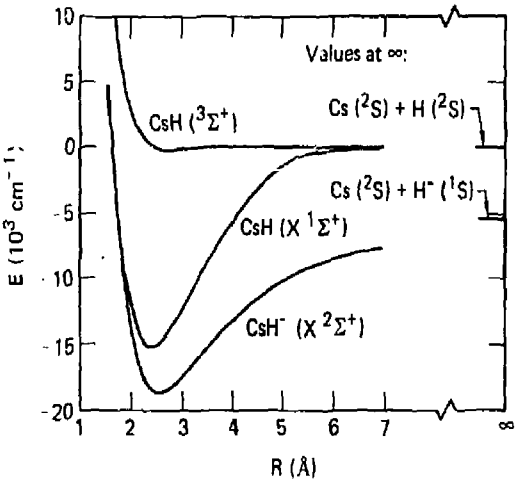
10
5
0
-5
-10
-15
-20
E (10^3 cm^{-1})
1
2
3
4
5
6
7
∞
R (Å)
Values at ∞:
Cs (^{2}S) + H (^{2}S)
Cs (^{2}S) + H$^-$ (^{1}S)
CsH ($^3\Sigma^+$)
CsH (X $^1\Sigma^+$)
CsH$^-$ (X $^2\Sigma^+$)

Figure 5

CsH respectively. These numbers are significantly larger than those for LiH and NaH, but this is not unreasonable since there is a large increase in the alkali polarizabilities in going from Na to K, and the polarizabilities dominate the attractive part of the anion potential-energy curves.

C. SUMMARY AND DISCUSSION

All of the molecular anion ground state potentials are found to be attractive and to lie below the neutral parent-hydride potentials over the internuclear distances examined, except for the CsH-CsH^- system. Because the Group IIA atom ground states, which are the united atom states for the alkali hydrides, are not expected to have stable anions, crossing of the alkali hydride neutral and anion curves is expected to occur somewhere on the left hand limbs.

Each alkali-hydride anion has a value of R_e from 5 to 7% larger than its neutral parent, and the negative-ion well depths range from 16% (for CsH^-) to 23% (for NaH^-) less than those of their respective neutral parents. These results are remarkably consistent with earlier ab initio results for the lithium, sodium, and cesium systems,[3] indicating that we have improved the neutral and negative ion results to about the same extent in our pseudopotential treatment.

Two interpretive descriptions of the anion molecular structure are possible. The first is to consider an electron attaching to the neutral molecule. The electron goes almost completely into a "non-bonding" orbital localized on the alkali atom while, at the same time, the principal bonding orbital becomes more localized on the hydrogen atom (i.e., becomes more non-bonding). This gives a qualitative explanation of the increased R_e and decreased D_e compared to the neutral. Alternatively, one can consider the anion as consisting of a highly-polarized alkali atom in the presence of H^-. This description holds over the entire range of internuclear separations. The charge-induced interactions are considerably weaker than the covalent bonding and charge-transfer interactions which dominate the neutral molecule.

Figure 6 (taken from Figs 4 and 5 of Ref. 3) shows the total electron density contours for LiH^- and CsH^- with those of LiH and CsH overlaid as shaded portions. The localization of the additional electron behind the alkali atom is readily apparent. It is this localization, combined with the corresponding limited change in correlation energy and orbital relaxation as the electron goes to the (electrostatically) favored region in the highly ionic neutral molecule, that makes it possible for a relatively limited configuration-interaction calculation to give satisfactory results - provided that the orbital basis sets are capable of describing the diffuse, polarized nature of the added electron.

All of the computed values of the equilibrium distance for the neutral molecules are somewhat smaller than the experimental values, ranging from a few tenths of a percent for NaH and KH to around 1% for LiH and 3% for RbH and CsH. These differences are consistent with the intrinsic accuracy of our calculations. The computed binding energies for the neutral molecules are in satisfactory agreement with experiment, the differences ranging from around 1400 cm^{-1} for LiH to 400 cm^{-1} for CsH. However, as we have noted, the closer agreement shown for the heavier systems is due principally to canceling errors that give the appearance of greater accuracy. For the series the accuracy of the calculations averages out to about 1000 cm^{-1}. Some improvement in the theoretical results will come from including appropriate terms in the orbital basis sets that will improve the calculated polarizabilities. Such an improved basis, coupled with a more extended configuration interaction, could be expected to improve the accuracy considerably over most of the region where core-core polarization effects are small. As discussed earlier, accuracy will be improved at smaller internuclear separations when corrections such as those described by Bottcher and Dalgarno[7] are included in the theoretical treatment.

Summarizing our results for the molecular electron affinities, we find a molecular electron affinity of 0.293eV for LiH. This value is obtained by adding the energy difference between the computed and experimental electron affinities for H (0.089eV) to the energy

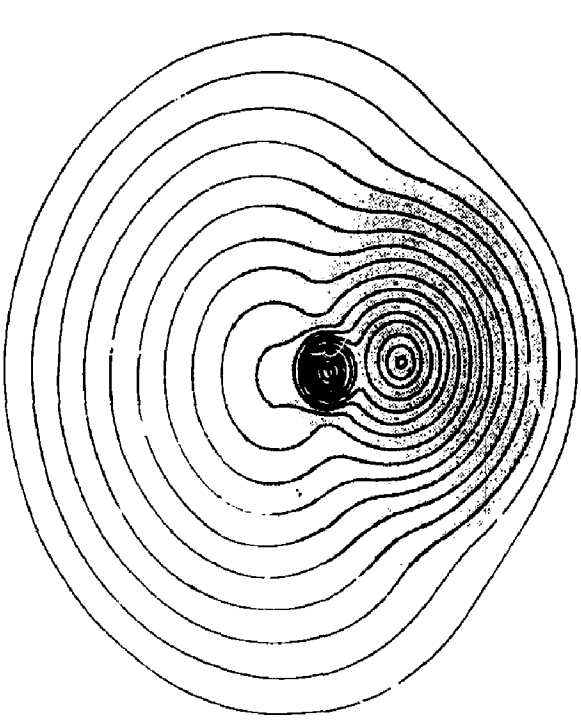

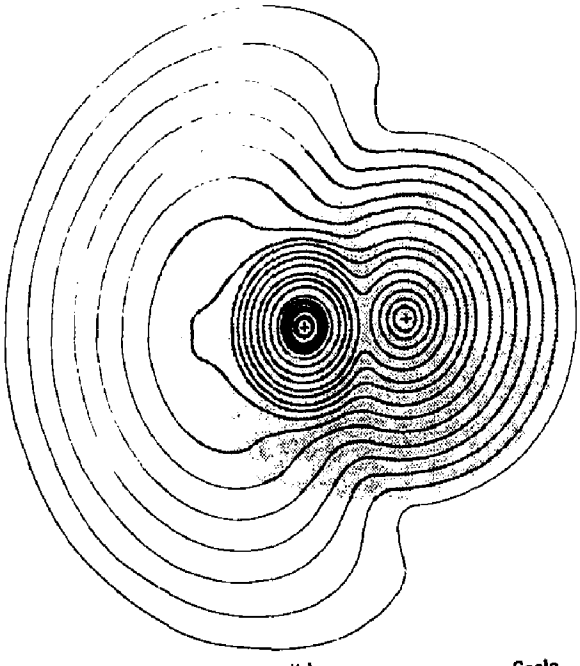

Figure 6

difference between the neutral and negative-ion potentials at their respective minima. Because of the well-characterized charge localization in the molecule, this correction should be largely invariant over a wide range of LiH^- internuclear distances including the region around the equilibrium separation. With additional polarization functions added to the basis, the electron affinity is found to be 0.33eV. These electron affinities are to be compared with our ab initio value of 0.283eV, the value of 0.2986eV determine by Griffing and Simons from their equation-of-motion calculations, and with the value of 0.32eV and 0.26eV obtained by LOD[11] and RM[15], respectively. For the remaining alkali hydrides the affinities range from 0.316eV for NaH to 0.438eV for CsH. Improved polarization basis set calculations have not been carried out for these molecules, but changes could easily be greater for the more polarizable heavy systems.

The molecular electron affinities, after adding the asymptotic energy shift, have been plotted in Fig. 7. All of the E.A. versus R plots are seen to go through a maximum at distances greater than R_e as predicted by our previous all-electron calculations.[3] This is consistent with the fact that the neutral interaction is dominated by charge overlap effects while the anion interaction is charge-induced multipole, and hence much longer range.

III. MOLECULAR DYNAMICS, ELECTRON-VOLUME PROCESSES, AND VIBRATIONAL DE-EXCITATION

We have now discussed procedures for obtaining the accurate potential curves needed for understanding the physical processes occurring in double-charge exchange processes and in plasma-surface interactions. We now turn our attention to electron-volume processes and specifically the problem of collisional de-excitation of vibrationally excited molecular hydrogen at an Fe surface. Here again the interaction potential plays a central role.

It has been shown in the study of electron-molecule collisions occurring in hydrogen discharges that the negative ion density increases with the third power of the electron density.(23) A realistic scenario

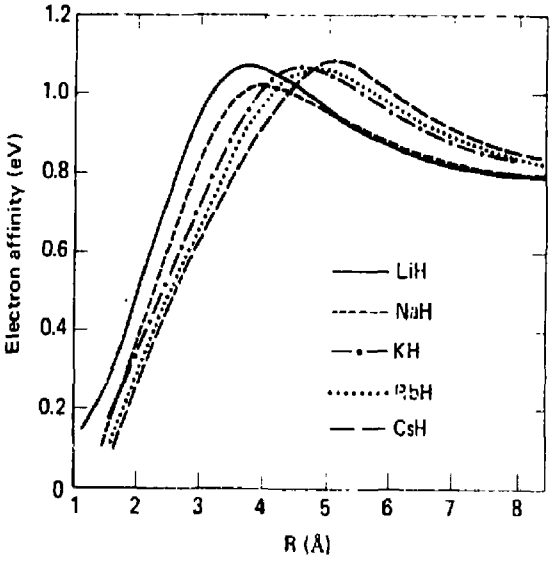
1.2
1.0
0.8
0.6
0.4
0.2
0
Electron affinity (eV)
1
2
3
4
5
6
7
8
R (Å)
LiH
NaH
KH
RbH
CsH

Figure 7

for the enhanced negative ion concentration is the following:

H_2^+, H_3^+ Production:

$$e + H_2 (v = o) \rightarrow H_2^+ (v) + 2e \quad (1)$$

$$H_2^+ (v) + H_2 (v = o) \rightarrow H_3^+ (v) + H \quad (2)$$

Auger Neutralization by Wall Collisions:

$$H_2^+ (v) + M \rightarrow H_2 (v \geqslant 6) + M \quad (3)$$

$$H_3^+ (v) + M \rightarrow H_2 (v \geqslant 6) + M \quad (4)$$

Excitation by e; Radiative Decay:

$$e + H_2 (v = o) \rightarrow e + H_2^* \rightarrow e + h\nu + H_2 (v \geqslant 6) \quad (5)$$

Dissociative Recombination:

$$e + H_3^+ (v) \rightarrow H_2 (v \geqslant 6) + H \quad (6)$$

Dissociative Attachment:

$$e + H_2 (v \geqslant 6) \rightarrow H_2^- \rightarrow H^- + H \quad (7)$$

Survival:

$$H_2 (v \geqslant 6) + M \rightarrow H_2 (v \geqslant 6) + M \quad (8)$$

$$H_2 (v) + M \rightarrow H_2 (v - 1) + M \quad (9)$$

The processes (1) and (2) lead to H_3^+ and H_2^+ fractions in hydrogen discharges of the order of 90 percent and 5 percent, respectively. Auger neutralization of H_2^+ and H_3^+ ions in wall collisions, shown in (3) and (4), the excitation from the ground state of hydrogen to higher singlet states by energetic electrons followed by radiative decay to the ground electronic state, indicated in (5), and the process of dissociative recombination, indicated in (6), are known to have large cross sections.[24-27] These are processes giving rise to the vibrationally excited molecules, $H_2(v)$. Kuiander and

Guest[28] have studied the products formed in step (6) and have concluded that the hydrogen molecules are formed with a substantial fraction in the higher vibrational states. It has been estimated that Auger neutralization of H_2^+ and H_3^+ ions in wall collisions may yield populations for levels $v > 6$ which are greater than 30 percent of the total $H_2(v)$ distribution.[24]

Careful analysis indicates that the most probable process for the production of H^- negative ions is the dissociative attachment to vibrationally excited hydrogen molecules indicated in step (7).[24] Cross sections greater than 2×10^{-16} cm^2 have been estimated[24,29] for both $H_2(v)$ and $D_2(v)$ for the upper levels $v \geq 9$. However, for the density of $H_2(v \geq 6)$ to rise sufficiently high for steps (1) through (9) to represent a credible scenario for explaining the observed negative ion yields, the vibrationally excited molecules must survive from 10 to 20 wall collisions, step (8), before vibrational de-excitation occurs, as shown in step (9).

In order to obtain insight into the transient response of vibrationally excited H_2 and D_2 to a collision with an appropriate surface and to estimate at least qualitatively the probability of survival of these highly excited molecules as a function of the number of wall collisions and the residence time near the surface, we have carried out computer experiments based on the method of molecular dynamics. An advantage of this technique is that it allows us to begin with simple approximations and gradually to refine the calculations as our understanding of the problem increases.

A. MOLECULAR DYNAMICS

Molecular dynamics has evolved rapidly to a sophisticated level because of the dramatic revolution in computer technology. It provides a powerful method for examining the microscopic details of a wide variety of phenomena. Briefly summarized, molecular dynamics involves the numerical solution by computer of Newton's equations of motion for all atoms comprising the active region of the assembly, thus giving the coordinates and velocities of the particles as a function

of time.[30] The set of coupled nonlinear second-order differential equations that represent the forces acting on the particles are reduced to a doubled set of first-order ordinary differential equations by standard procedures. The initial positions and velocities of the particles represent the initial conditions on these equations. Practical limits on the number of particles in a given ensemble currently are in the range of 10^3 to 10^4, and periods of time during which the evolution of the system can be followed range from 10^3 to 10^4 in units of time natural to the problem being considered. Molecular vibration frequencies are typically of the order of 10^2 to 10^3 cm^{-1}, and correspond to vibrational periods of tenths to hundredths of picoseconds (10^{-12} seconds). Rotational periods are usually around a hundred times longer. In general, simulations requiring a few minutes of computer time allow us to examine the real-time evolution of a given system for up to several hundred picoseconds. Within these constraints an almost unlimited variety of computer simulations can be explored.

B. MOLECULE-WALL SIMULATION STUDIES

1. Initial Conditions and Dimensionality

The study of energy transport and decay in discrete systems can be carried out in two-dimensional systems as well as in three-dimensional, "more realistic" situations. Although care must be exercised in allowing for the purely two-dimensional character of the results, such studies can lead to valuable insights and the general characteristics of an evolving system can be observed with minimal expenditure of computer time.

Three-dimensional lattices are inherently more realistic, with the increased dimensionality adding translational, vibrational, and rotational degrees of freedom and opening channels for relaxation processes not otherwise present in two-dimensional systems. For the rather simple situation we are looking at here, it is very possible, however, that the general features we see in the two-dimensional

calculations contain almost all of the qualitative information that will be found in the three-dimensional simulations.

Surfaces with which the molecule will interact can be constructed with irregularities and with variations in mass and potential. Questions that can be given detailed examination include the nature of the particle-surface interaction as a function of different initial conditions; the general nature of interparticle momentum transfer and its dependence on the effective interaction potential; the stability of the vibrotational state of the molecule and its dependence on the discrete nature of the mass array in the wall; and the importance of the nonlinear, or chemical, nature of the interatomic forces.

For our molecule-wall simulation studies initial conditions for the computer experiment include: variations of temperature and temperature gradient of the wall; detailed specification of the particle, its internal modes, and its interaction with the wall (e.g., the isotopic composition, the vibrotational excitation, and the velocity and impact angle of the molecule with the wall); and the crystallographic orientation and the type of lattice simulated. Figure 8 depicts a typical starting configuration for a computer run. Parameters given specific initial values are the incident angle θ, the distance from the surface, the center of mass velocity, the surface temperature T, and the initial vibrational and rotational energies corresponding to a (classical) specification of the quantum numbers v and J. The phase angle α and impact point on the surface are randomly chosen.

2. Potentials

The force acting on any one particle in the ensemble is the resultant of all interactions with other atoms in its neighborhood and is obtained as a derivative of an effective many-body potential. However, any molecular dynamics calculation which would in fact attempt to include most or all of a complete potential energy hyper-surface represents a Herculean task far beyond present considerations. Fortunately, our experience to date indicates that much can be learned within the framework of a suitably generalized pair-potential approximation. In going beyond this simple treatment at some later

stage, we are likely to find it possible to deal only with those portions of the hyper-surface that are relevant to the trajectories of the particle and the chemical dynamics of the evolving system. The two-body potential for FeH has been adapted from the work of Scott and Richards,[31] and unpublished work on Fe_4H clusters[32] and the Fe potential from the two-body potential derived by Johnson[33] in which experimental elastic-constant data were used. For the molecular dynamics simulations we are reporting here, these two-body potentials form the framework within which the interrelated particle and chemical dynamics of the system must be described.

C. CALCULATIONS

In these initial calculations we consider simple two-dimensional simulations of the type depicted in Fig. 8. At some initial time, t = 0 (in units of 10^{-14} seconds), a hydrogen molecule is set in motion toward a lattice composed of iron atoms. We have chosen a (110) plane of the body-centered cubic phase of Fe for these initial computer studies, as this particular two-dimensional configuration most closely matches the lattice used in extensive shock propagation studies carried out for two-dimensional face-centered cubic structures.[34] At the time, t = 21, of Fig. 9 the molecule has approached near enough to the surface for long-range interactions to be included in the equations of motion.

The initial translational velocity of the H_2 molecule has been chosen equal to the average molecular speed associated with a gas temperature of 500K; at this temperature the J = 1 rotational state also predominates. In most of our computer runs, the initial vibrational energy is that associated with the v = 8 vibrational level, about 28,000 cm^{-1} above the potential energy minimum. For the v = 8 level, a Morse curve fit predicts the left turning point to be at 0.423 A and the right turning point to be at 1.757 A. For the wall, the Fe atoms have been given initial thermal motion characteristic of a temperature of 500K. Because of the small number of atoms comprising the wall, this is more properly related to a local kinetic temperature rather than a true thermodynamic temperature. For the dynamics of our problem, this distinction is not important. In the equations of motion, masses are in atomic mass units, and the units of time are in 10^{-14} seconds.

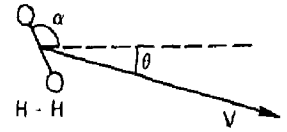

$E_{TOT} = E_{TRANS} + E_{VIB} + E_{ROT}$

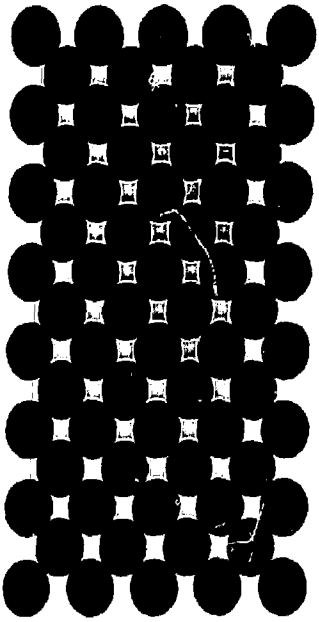

Wall: Cu, Ti, W, Mo, Fe

Parameters:

- E_{TRANS}, E_{VIB}, E_{ROT}
- θ, α
- Position of impact
- Temperature of wall

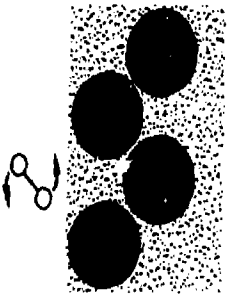

Figure 8

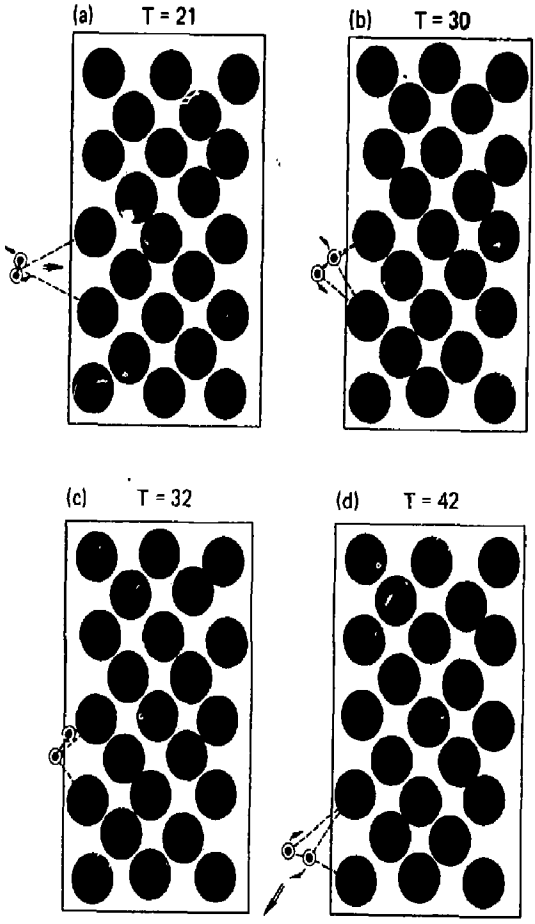

Figure 9

D. DISCUSSION

1. Single-Trajectory Dynamics

It is rather instructive to follow one example in some detail. In Fig. 9a, the molecule is shown moving toward the wall at the time, t = 21 (21 x 10^{-14} seconds) just as it has begun to interact with the wall. Before interaction, its vibrational excitation is equivalent to a molecule in the v = 6 level, with rotational motion characteristic of the J = 1 level. The interaction at t = 21 is very weak and is depicted by dashed lines indicating those bonds which the code itself recognizes as having been formed between the hydrogen atoms and the iron atoms of the wall. The two hydrogen atoms are seen to be momentarily near the inner turning point, i.e., in the close-in or helium-like configuration. In Fig. 9b, the molecule has approached quite near the surface; the code now recognizes additional, but rather weak, bonding. At the moment shown in Fig. 9b, the molecule is in a stretched or hydrogen-atom-like configuration, so that the potential appropriate for the Fe-H interaction is the weak, long-range part of the Fe-H pair potential. Rapid changes in electronic structure now occur associated with the rapidly varying spatial positions, and at t = 32, shown in Fig. 9c, a strong bond has formed between one of the hydrogen atoms and an Fe surface atom, all other interactions remaining weak. The result of a sequence of strong dynamical interactions occurring between t = 32 and t = 40 is shown in Fig. 9d where the molecule is now moving away from the surface, with only a few weak, long-range bonds remaining, indicating a rapidly diminishing interaction with the surface.

As we follow the motion of the molecule near the surface, we monitor a number of interesting dynamical quantities, some of which are shown in Fig. 10. When the molecule is far from the surface, we are able to factor its internal energy into rotational and vibrational kinetic energy and vibrational potential energy. The translational motion is also calculated and the sum of these energies, or the total energy of the molecular unit, is plotted. We have also found that plotting the center-of-mass position relative to the surface provides

not only information about the position and velocity of approach of the molecule with respect to the wall but also provides very useful information about the "residence time" near the surface. As the molecule nears the surface, changes in the translational kinetic energy can be seen as well as changes in the slope of the center-of-mass plot. During the time of strong interaction with the surface, the molecular vibrational and rotational energies are not necessarily well-defined. These quantities should only be used as a vivid indication of the rapidly varying dynamics occurring at the surface. As the molecule leaves the surface, changes in these quantities from values possessed by the incoming particle can be calculated. For the example we have used in Fig. 9, we shown in Fig. 10 the corresponding dynamical quantities plotted from t = 24 to t = 44. During the collision with the wall, the initial vibrational energy of -2.50eV (the sum of the vibrational kinetic and potential energy components) decreases to around -3.25eV, but the molecule at the same time picks up both rotational and translational energy.[35] Overall, the total energy of the molecule has increased after collision with the wall. From Fig. 10, we can also see that the residence time of the hydrogen atoms at the surface for this collision was of the order of 7 - 8 x 10^{-14} seconds, i.e., from 7 to 8 vibrational periods for the isolated molecule in its v = 6 state. Subsequent collisions of this hot molecule with the wall will give rise to further changes in the vibrational and rotational energy. For any given collision with the wall, the molecule may pick up or lose vibrational, rotational, and translational energy. It is the statistical averaging of these events that will provide a more complete answer to the question of collisional de-excitation.

2. Average Properties of the System

It can be seen that single trajectories give us the detailed dynamics of individual events and insight into the microscopic details of individual collisions. We next consider the averaged behavior of a statistically significant number of trajectories in order to obtain results that correspond to macroscopic or physically-observable

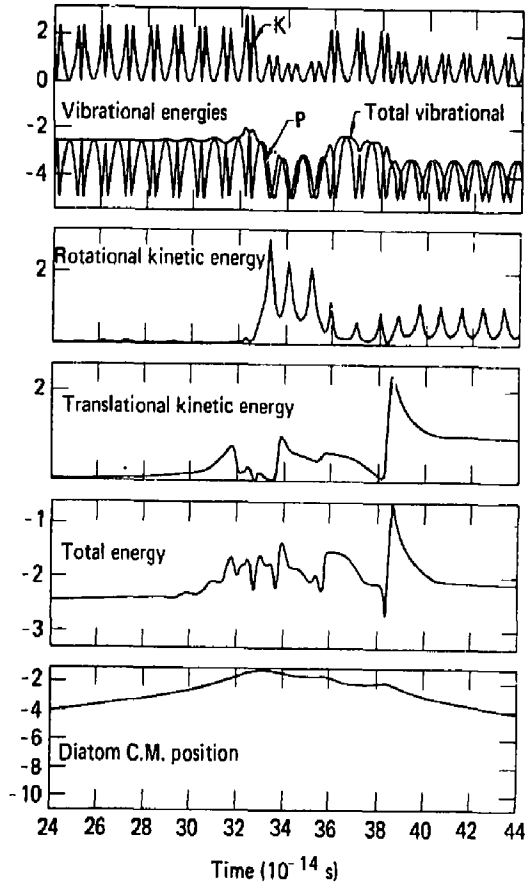
2
0
-2
-4
K
Vibrational energies
P
Total vibrational
2
Rotational kinetic energy
2
Translational kinetic energy
-1
-2
-3
Total energy
-2
-4
-6
-8
-10
Diatom C.M. position
24
26
28
30
32
34
36
38
40
42
44
Time (10^{-14} s)

Figure 10

behavior. These studies have initially focussed on the statistical, or average, loss or gain of vibrational, rotational, translational, and total energy of the H_2 molecule. We have also considered the average residence time, or time of interaction, of the molecule at the surface, since it appears plausible that this might affect to a considerable degree the probability of excitation or de-excitation.

In our calculations a computer "run" consists of a selected H_2 molecule colliding repeatedly with the wall for up to ten times unless capture or dissociation occurs. We then restart with a "new" H_2 molecule, until we have completed ten sets. Thus, each run consists of 100 trajectories, with 10 "first-bounce" collisions with the wall, 10 "second-bounce" interactions, and so on. We choose some specific initial trajectory angle with respect to the wall (30^0 for the example here) for each set of ten collisions with wall; after the first bounce in the series, the angles of approach will differ to the degree that the collision is non-specular. Although the initial trajectory angle in each set is specified, the phase angle α and impact point on the wall are chosen randomly.

In Fig. 11 we show an example of the results obtained for a rather limited group of 100 trajectories centered about a 30^0 angle of approach to the wall. Results for the average vibrational, rotational, and translational energy, as well as the sum or average total energy, are shown as a function of the "bounce" number (the number of times the molecule has collided with the wall). Although these results are very preliminary and many additional trajectories must be included in order to decrease the statistical fluctuations, we can observe the following:

(a) The total energy of the H_2 molecule, which was initially only vibrationally highly excited, remains high, with wall collisions providing an efficient mechanism for V-T and V-R energy transfer.

(b) Rotational excitation from the initial $J = 1$ state up through very large J values ($J \geq 14$) occurs in all cases and is exceedingly rapid.

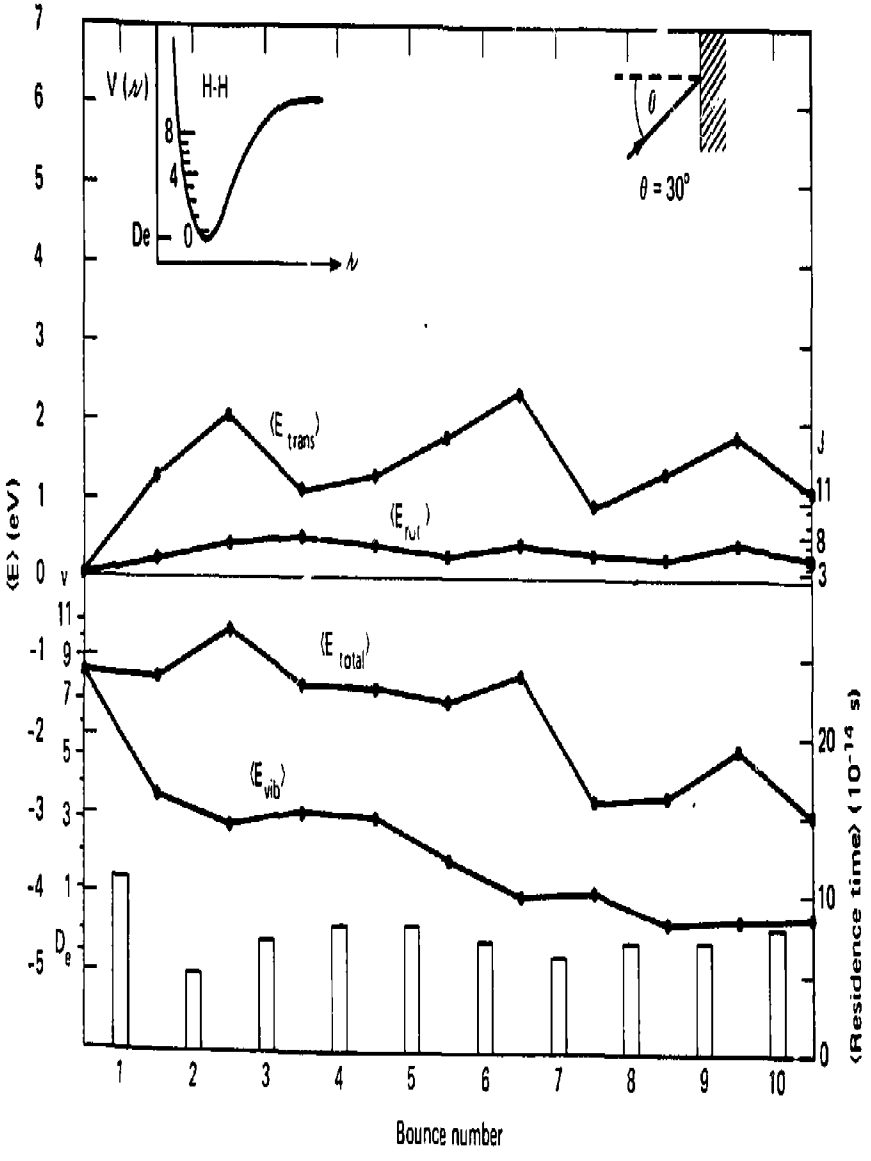
V(ν)
H-H
8
4
De
0
ν
θ
θ = 30°
⟨E⟩ (eV)
⟨E trans⟩
⟨E rot⟩
J
11
8
3
v
11
9
7
5
3
1
⟨E total⟩
⟨E vib⟩
De
⟨Residence time⟩ (10⁻¹⁴ s)
20
10
0
1
2
3
4
5
6
7
8
9
10
Bounce number

Figure 11

(c) Vibrational de-excitation is most marked during the first collision, before rotational excitation has taken place; during subsequent bounces, a significant fraction of trajectories result in vibrational re-excitation to intermediate vibrational states.

(d) The average residence time during the first bounce is significantly greater than for subsequent collisions and it would appear must be taken into account in order to understand V-T-R energy flow in molecular wall-collision events of the type we are considering. For the relatively weak average interaction potential used in our present example, the H_2 molecule in most collisions strongly interacts with the wall for only a few vibrational periods.

These observations are at once both tentative and suggestive. We need to proceed with additional statistical sampling and a careful analysis of the sensitivity of the results to the interaction potential. This work is actively in progress.

E. SUMMARY

In Section III we have discussed the application of computer molecular dynamics to an important technological area where experimental data may be very difficult to obtain: collisional de-excitation at surfaces of vibrationally highly excited molecular systems. Here our interest is specifically in H_2, D_2, and HD, vibrationally excited above the v = 6 level. We have illustrated the technique by means of a specific example and have demonstrated the detail that can be obtained from such calculations. We have also pointed out the need to characterize as realistically as possible the effective potentials, and therefore the resulting forces, as the molecular species approach and interact with the surface. In addition, we have indicated the necessity of sampling and averaging the results of many trajectory runs in order to arrive at meaningful conclusions about the probability of de-excitation as a function of the number of wall collisions, the

incidence angle and impact point, the residence time, the wall temperature, and the nature of the wall itself. Finally, results obtained from two-dimensional simulations will have to be compared with three-dimensional trajectory calculations to remove uncertainties about a two-dimensional bias in the results.

ACKNOWLEDGMENTS

The MCSCF pseudopotential calculations were carried out in collaboration with Walter J. Stevens, National Bureau of Standards, and will be reported in more detail in a forthcoming journal article.[36] The vibrational de-excitation studies represent part of a collaboration with John R. Hardy and Robert J. Hardy, University of Nebraska, in the application of molecular dynamics to heterogeneous systems. Thanks are due also to Thomas M. DeBoni, Lawrence Livermore National Laboratory, for developing the molecular dynamics computer codes and for help in carrying out the calculations. Finally, the author is indebted to John R. Hiskes for many helpful and stimulating discussions of this work.

Figure Captions

Figure 1. Potential energy curves for LiH and LiH^-. Solid line = this work. Dashed line = Liu, Ohata, and Docken (Ref. 11). The negative ion potentials have been shifted to dissociate to the correct experimental asymptote.

Figure 2. Potential energy curves for NaH and NaH^-. Solid line = this work. Dashed line = Olson and Liu (Ref. 5). The negative ion potentials have been shifted to dissociate to the correct experimental asymptote.

Figure 3. Potential energy curves for KH and KH^-. The negative ion potential has been shifted to dissociate to the correct experimental asymptote.

Figure 4. Potential energy curves for RbH and RbH^-. The negative ion potential has been shifted to dissociate to the correct experimental asymptote.

Figure 5. Potential energy curves for CsH and CsH^-. The negative ion potential has been shifted to dissociate the correct experimental asymptote.

Figure 6. Total molecular charge density comtours for:
(a) LiH^- $^2\Sigma^+$ state with LiH $^1\Sigma^+$ state superimposed as shaded portion.
(b) CsH^- $^2\Sigma^+$ state with CsH $^1\Sigma^+$ state superimposed as shaded portion.
Distances are in bohrs and densities are in electrons/(bohr).^{3} The innermost contour value for (a) is 1.0 and for (b) is 16.0 and the ratio between successive contour values is 1/2. This figure is taken from Figs. 4b and 5b of Ref. 3.

Figure 7. Calculated electron affinities of the alkali hydrides as a function of internuclear separation. Uniform corrections have been added to yield the experimental hydrogen affinity.

Figure 8. Typical starting configuration for computer simulation of an H_2 molecule moving toward a wall at velocity v and angle . Close encounter with the wall is shown in the inset.

Figure 9. Configurations of an H_2 ($v = 6$, $J = 1$) molecule within range of interaction with a lattice composed of Fe atoms: (a) the H_2 molecule near its inner turning point; weak, long-range interactions are shown by dashed lines; (b) the molecule near its outer turning point; additional long-range, weak interactions are present; (c) the molecule near the Fe surface; a strong chemical bond has formed as indicated by the solid line; and (d) the molecule moving away from the surface with only weak, long-range interactions remaining. The time t is shown in each figure.

Figure 10. Vibrational, rotational, and translational energies, and the center-of-mass distance normal to the surface plotted against time for the trajectory described in Fig. 9. The vibrational energy has been additionally separated into its kinetic and potential energy components, and the total molecular energy has been plotted.

Figure 11. Average values for the vibrational, rotational, translational, and total energies as a function of bounce number for the computer run described in the text. The trajectories are clustered around a 30^{o} approach to the wall, as shown in the inset. Also shown is a schematic of the H_2 molecular potential indicating the positions of the vibrational levels up to v = 8. Average residence times associated with the bounces are shown along the bottom of the figure.

REFERENCES

1. Y. I. Belchenko, G. I. Dimov, and V. G. Dudnikov, Proc. of the Second Symposium on Ion Sources and Formation of Ion Beams, Lawrence Berkeley Laboratory Report No. LBL-3399, October 1974.

2. J. R. Hiskes, A. M. Karo, and M. A. Gardner, J. Appl. Phys. 47, 3888 (1976).

3. A. M. Karo, M. A. Gardner, and J. R. Hiskes, J. Chem. Phys. 68, 1942 (1978).

4. K. M. Griffing J. Kenney, J. Simons and K. D. Jordan, J. Chem. Phys. 63, 4073 (1975).

5. R. E. Olson and B. Liu, J. Chem. Phys. 73, 2817 (1980).

6. J. N. Bardsley, Case Studies in Atomic Physics 4, 299 (1974); Chem. Phys. Lett. 7, 517 (1970).

7. C. Bottcher and A. Dalgarno, Proc. Roy. Soc. A340, 187 (1974).

8. W. J. Stevens, J. Chem. Phys. 72, 1536 (1980).

9. G. Das and A. C. Wahl, "BISON-MC: A FORTRAN Computing System for Multiconfiguration Self-Consistent-Field Calculations on Atoms, Diatoms, and Polyatoms," Argonne National Laboratory Report No. ANL-7955 (1972).

10. K. C. Li and W. C. Stwalley, J. Chem. Phys. 70, 1736 (1979).

11. B. Liu, K. O. Ohata, and K. K. Docken, J. Chem. Phys. 67, 1850 (1977).

12. P. Rosmus and W. Meyer, J. Chem. Phys. 63, 2356 (1975).

13. K. K. Docken and J. Hinze, J. Chem. Phys. 57, 4928 (1972).

14. K. R. Way and W. C. Stwalley, J. Chem. Phys. 59, 5298 (1973); K. C. Li and W. C. Stwalley, J. Mol. Spectrosc. 69, 294 (1978).

15. P. Rosmus and W. Meyer, J. Chem. Phys. 69, 2745 (1978).

16. K. D. Jordan, K. M. Griffing, J. Kenney, E. L. Andersen, and J. Simons, J. Chem. Phys. 64, 4730 (1976).

17. W. C. Stwalley, unpublished work.

18. F. B. Orth and W. C. Stwalley, J. Mol. Spectrosc. 79, 314 (1980).

19. S. C. Yang, Y. K. Hsieh, K. K. Verma, and W. C. Stwalley, J. Mol. Spectrosc. (to be published).

20. Y. K. Hsieh S. C. Yang, A. C. Tam, K. K. Verma, and W. C. Stwalley, J. Mol. Spectrosc. (to be published).

21. Y. K. Hsieh, S. C. Yang, A. C. Tam, and W. C. Stwalley, J. Chem. Phys. 68, 1448 (1978).

22. W. C. Stwalley, S. C. Yang, F. B. Orth, and K. C. Li, J. Chem. Phys. 69, 1791 (1978).

23. M. Bacal and G. W. Hamilton, Phys. Rev. Lett. 42, 1538 (1979).

24. J. R. Hiskes, J. de Physique, Colloque C7, Suppl. 7, 40, C7-179 (1979).

25. B. Peart and K. T. Dolder, J. Phys. B. 7, 1948 (1974).

26. M. Bacal, I. M. Bruneteau, W. G. Graham, G. W. Hamilton, and M. Nachman, J. Appl. Phys. (to be published).

27. J. R. Hiskes, J. Appl. Phys. 51. 4592 (1980).

28. K. C. Kulander and M. F. Guest, J. Phys. B 12, L501 (1979).

29. J. M. Wadehra and J. N. Bardsley, Phys. Rev. Lett. 41, 1795 (1978).

30. B. J. Alder and T. E. Wainwright, J. Chem. Phys. 27, 1208 (1957); 31, 459 (1959); 33, 1439 (1960).

31. P. R. Scott and W. G. Richards, J. Chem. Phys. 63, 1690 (1975).

32. R. L. Jaffee, private communication.

33. R. A. Johnson, Phys. Rev. 134A, 1329 (1964).

34. A. M. Karo and J. R. Hardy, Proc. of the NATO Advanced Study Institute on Fast Reactions in Energetic Systems, Ioannina, Greece, 1980, edited by C. Capellos and R. Walker (D. Reidel Publishing Co., Dordrecht-Holland, Boston-U.S.A., 1981).

35. The negative sign appears because, by convention, we define the asymptotic energy of the dissociated H_2 molecule to be zero. Our value for D_e for H_2 is -4.745 eV.

36. W. J. Stevens, A. M. Karo, and J. R. Hiskes, J. Chem. Phys., in press.